Astron. Astrophys. 322, 139–146 (1997)

ASTRONOMY AND ASTROPHYSICS

Observations of the recent disc loss in X Persei: photometry and polarimetry

P. Roche[1], V. Larionov[2], A.E. Tarasov[3], J. Fabregat[4], J.S. Clark[5], M.J. Coe[5], P. Kalv[6], L. Larionova[2], I. Negueruela[5], A. J. Norton[7], and P. Reig[4]

[1] Astronomy Centre, CPES, Sussex University, Falmer, Brighton BN1 9QH, UK
[2] Astronomical Institute, St.Petersburg University, 198904 St. Petersburg, Russia
[3] Crimean Astrophysical Observatory, 334413 Nauchny, Crimea, Ukraine
[4] Departamento de Astronomía, Universidad de Valencia, E-46100 Burjassot, Valencia, Spain
[5] Astronomy Group, Physics Department, Southampton University, Southampton SO17 1BJ, UK
[6] Tallinn Observatory, Institute of Physics, Tallinn Technical University, Estonia
[7] Department of Physics, The Open University, Walton Hall, Milton Keynes MK7 6AA, UK

Received 2 May 1996 / Accepted 16 November 1996

Abstract. We present optical and infrared photometric observations of the Be/X-ray binary system X Persei/4U0352+30 during the past decade, covering the entire phase change from Be to OB star and back. Intrinsic colours are derived based on observations during the disk-less phase, giving E(B–V)=0.36±0.02, $(B–V)_0$=–0.22±0.02 and $(U–B)_0$=–1.05±0.02, suggesting a B0V star at a distance of 900pc±300pc and an extinction of A_v=1.16±0.03. We find evidence for only one variable component, presumed to be the disc. We present measurements of the intrinsic polarisation, and an estimate of the interstellar polarisation. Polarimetric observations reveal major changes in the degree of polarisation, indicating the reformation of a scattering envelope around the star, but these are inconsistent with the predictions of standard Be envelopes models, possibly as a result of geometrical effects.

Key words: stars: X Per – X-rays: stars – polarization – accretion disks

1. Introduction

X Persei (HD 24534) is the optical counterpart to the pulsating X-ray source 4U0352+30 (Braes & Miley 1972; van den Bergh 1972; Brucato & Kristian 1972; Weisskopf et al. 1984), originally thought to be an O9.5IIIe star at a distance of 1300pc, with a magnetised neutron star companion (period ≈835 secs.) (White et al. 1976; Robba & Warwick 1989). Recent spectroscopic observations reported by Lyubimkov et al. (1996) have reclassified the system as B0Ve, with a revised distance of around 700±300pc. X Per is thus a member of the Be/X-ray (BeXRB) subclass of massive X-ray Binaries, although it is unusual in that it does not appear to display X-ray outbursts.

Earlier papers presented observations showing that X Per lost it's circumstellar disc and reverted to a "normal" OB-type star during 1989–1990 (Norton et al. 1991, henceforth N91; Fabregat et al. 1992, henceforth F92). Roche et al. (1993, henceforth R93) discussed the recent phase change in more detail, and presented evidence for a similar "extended low state" (ELS) during 1974–1977. We have subsequently monitored X Per, and present here observations spanning the onset of a shell-type emission profile at Hα (October 1991; Corbet & Thomas 1991), the gradual return to the full Be state, the fading event which followed it and the development of a second, inner circumstellar disc (Tarasov & Roche 1995).

X Per has been intensely monitored in the optical and infrared throughout the recent phase change, providing a unique dataset of this event. In view of the size of the dataset available to us, we present our observational data in several papers, this one dealing with the optical and IR photometric and polarimetric observations - future papers will discuss optical spectroscopy (Roche et al. 1996), IR spectroscopy (Clark et al. 1996), and modelling of the disc (Telting et al. 1996).

2. Photometric observations

2.1. Sources of photometric data

We present here an optical and infrared photometric history of X Per spanning the last ≈10 years, covering the entire phase change and the precursor optical bright state. The dataset includes that used in R93 and references therein, new observations summarised in Table 1, published data from Kunjaya & Hirata (1995; henceforth KH95), Zamanov & Zamanova (1995), Heng-rong & Zhi-run (1994), and CCD and photo-electric ob-

Send offprint requests to: P. Roche (pdr@star.maps.susx.ac.uk)

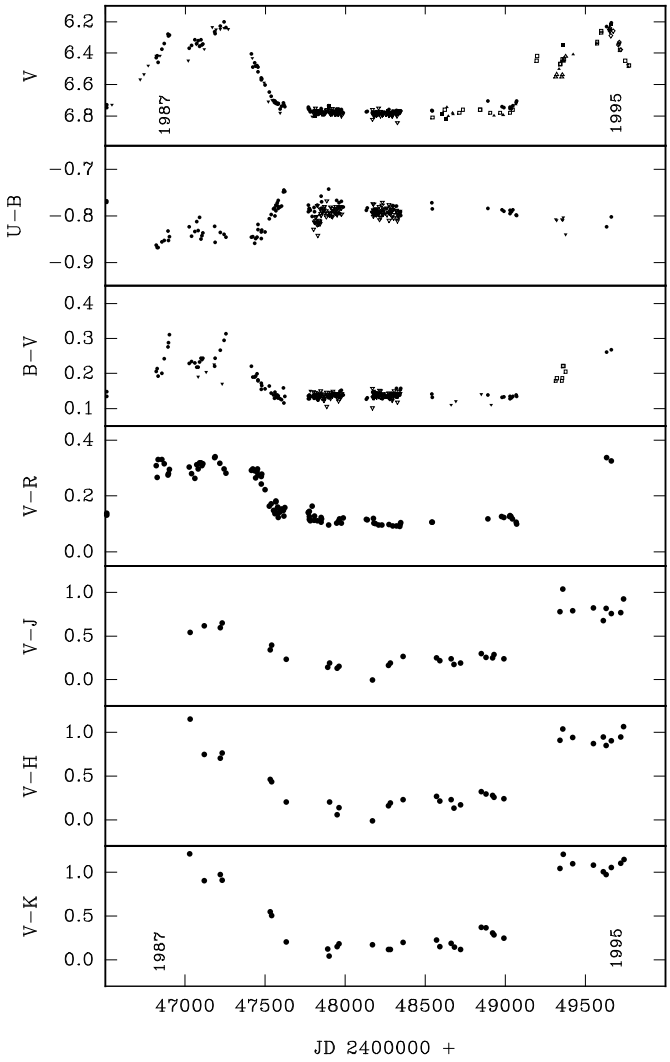

Fig. 1. The optical and infrared behaviour of X Per from 1985-1995.

servations from the British Astronomical Association Variable Star Section (BAA VSS).

Table 1 includes details of the new observations, with the check and comparison stars listed. Data obtained in the Stromgren narrow band system has been converted to standard Johnson bands using the transformations of Turner (1990). The infrared data were reduced using a number of standards obtained each night.

Due to the variety of optical data sources and photometric systems, combining these datasets required the application of small systematic corrections, to produce consistent lightcurves and colour diagrams. The Tallinn Observatory data were taken as the baseline for this procedure, as they covered the longest timespan and were in close agreement with the photometry of Percy (1992) and the binned V band lightcurve from R93. The infrared data from Byurakan and Izana Observatory were found to be consistent, and no correction was applied.

Table 1. Observational details, optical and IR photometry

Date of Observation(s)	No. of Observations	Bands	Telescope
Nov. 1990–Sep. 1993	3	*uvbyβ*	ALM
Feb. 1992–Nov. 1992	4	UBVRI	JKT
Dec. 1992–Dec. 1993	13	UBVRI	CAO1
Aug. 1987–Sep. 1991	43	UBV	SPU
Mar. 1987–July 1991	78	RI	SPU
Jan. 1974–Nov. 1994	240	UBV	TO
Aug. 1987–Oct. 1990	30	JHK	BO
Nov. 1987–Sep. 1995	55	JHKL′	TCS
Dec. 1993–Sep. 1995	19	JHKL	CAO2

Notes for Table 1:

ALM: 1.5m Calar Alto Observatory, Almeria, Spain. Single channel photometer. Various standards throughout night.
JKT: 1m Jacobus Kapteyn Telescope, Isaac Newton Group, La Palma, Canary Islands. CCD photometry. Standards HD24167, 97z351, 114z750.
CAO1 : 1.25m Crimean Astrophysical Observatory, Ukraine. UBVRI photometer-polarimeter. Standard HD24167.
CAO2 : 0.74m Crimean Astrophysical Observatory, Ukraine. Single channel InSb photometer. Standard Zeta Per.
SPU: 0.5m St. Petersburg University Observatory, Byurakan, Armenia. Single channel photometer.
TO: 0.5m Tallinn Observatory, Tallinn Technical University, Estonia. EMI 9502 and FEU-79 photomultiplier tubes. Standards GC4516, GC4548.
BO: 2.6m Byurakan Observatory, Byurakan, Armenia. St.Petersburg University IR photometer with PbS photoconductor.
TCS: 1.5m Telescopio Carlos Sanchez, Izana Observatory, Tenerife, Canary Islands. Continuously Variable Filter. Various standards throughout night.

2.2. Optical photometry

Fig. 1 presents the optical and IR data covering 1985–1995. The V band data are the original data with correction factors where necessary, the colour plots use data in 20 day bins. Discussion of the spectroscopic data is left to Roche et al. (1996), but mention will be made where necessary of the development of the Hα line profile during the Be→B→Be transition where it is relevant to the behaviour of the photometry.

The V band lightcurve shows two maxima, one preceding the ELS and peaking around JD 2447250, the second following the ELS and reaching maximum around JD 2449700. Both display structure, the earlier maximum apparently having two peaks. The shape of the later maximum is difficult to define due to the unfortunate location of seasonal gaps in the lightcurve, but it may show evidence for multiple peak structure. Overall, both maxima appear very similar in shape, duration and maximum brightness (V≈6.2). The ELS displays no short term variability larger than ≈0.03 magnitudes (Percy 1992 suggests a limit of 0.01 mags. on V band variability), but there is a small long term trend showing a minimum around JD 2448000-2448500. This trend appears to reflect the Hα variability, with the minumum coinciding with the appearance of an absorption profile, and the

slow brightening after JD 2449000 matching the re-appearance of emission in Hα.

The (B–V) colour curve shows both maxima as being accompanied by significant reddening, Δ(B–V)$\approx$0.15, consistent with an increase in circumstellar material. It is interesting to note two apparent short term increases in (B–V) seen in the 1986–1989 maximum, coinciding with the photometric peaks. These features have an amplitude of $\approx$0.05 mags., and appear to last at least a month. There is insufficient data in the current maximum to say whether such events have occurred. No such features are seen in the (U–B) colour curve in either maximum.

Once again, the ELS is marked by a lack of variability in (B–V) and (U–B) colours, as the scatter in (U–B) may be instrumental only. The (U–B) colour curve shows a relatively rapid linear increase from JD 2447450–2447700, coincident with the linear fade in the V band. The amplitude of (U–B) variability is $\approx$0.06 mags. over a period of $\approx$300 days. During the V band fade into the ELS, the (B–V) colour decreases to a minimum value of 0.14. Following the ELS, the system slowly becomes redder over the period JD 2449100 to 2449700, a much more gradual increase than that observed in the V band.

The Hα changes will be discussed more fully in Roche et al. (1996), but here we will comment on the general behaviour of the line. During the 1986–1989 maximum, the line has a strong, V-wing dominated profile. As the system fades, the line weakens (R93), and during the ELS the line reverts to absorption. In late 1991, the first signs of emission re-appear (Corbet & Thomas 1991), and the line gradually returns to a double-peaked profile as X Per brightens. However, at maximum brightness in 1994, the line is still significantly weaker, and of different shape, than was seen during the 1986–1989 maximum. Unusual changes observed in spectral lines following the recent maximum are discussed by Tarasov & Roche (1995), where the HeI $\lambda\lambda$ 6678Å line is observed with a four component structure that may indicate the development of a new hot, inner disc within the disc which formed at the end of the ELS. This structure has persisted for at least 18 months after its discovery in Feb. 1995.

In summary, the recent optical photometric history of X Per shows a period of slow brightening (1986 to 1988), showing short term variations of brightness and colour, followed by a relatively rapid fade (during 1989) which marks the onset of the ELS. The ELS shows no apparent variability, and is marked by the bluest colours observed for X Per. The ELS ends with a gradual brightening during 1993–1994. The system reached maximum brightness in late 1994, and has subsequently entered another period of relatively rapid fading, at a similar rate to that seen in 1989.

2.3. Infrared photometry

It can be seen from the lower panels of Fig. 1 that the incomplete IR coverage precludes discussion of all but the general behaviour of the system. All the lightcurves show a similar pattern, with a relatively rapid fade coincident with that seen in the optical, but with greater amplitude: ΔJ=1.3 mags., ΔH=1.5, ΔK=1.7, ΔL=1.6.

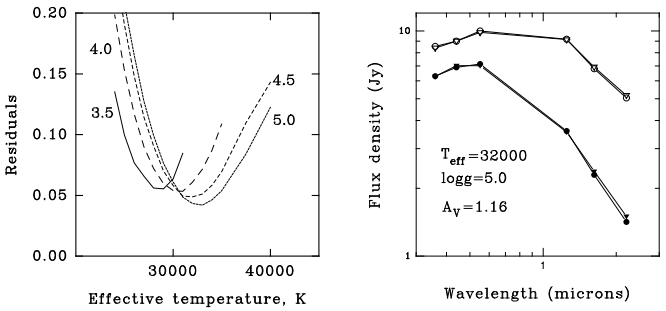

Fig. 2. Best fit for the observed X Per fluxes in the UBVJHK bands and standard Kurucz model atmospheres. Circles represent observed points (closed circles from ELS, open from maxima), and triangles represent the corresponding best fit Kurucz model with the addition of the excess emission attributed to the circumstellar envelope.

The ELS displays no large scale variability in our dataset, and ends with a gradual increase in brightness, peaking around JD 2449700, in agreement with the optical data. This recent maximum is of comparable brightness, in all infrared bands, to the 1986–1989 maximum.

3. Determination of the intrinsic colours, extinction and flux distribution

3.1. Extinction

Using the UBVJHK photometry obtained in the ELS and at optical maxima, we now derive an estimate for the extinction to X Per by fitting Kurucz model stellar atmospheres (Kurucz 1979, 1993) to the observed fluxes. Clearly, the value of A_v will be dependent on the physical parameters assumed for X Per (T_{eff} and log g), and we show in Fig. 2 the best fit obtained for models ranging from T_{eff} = 26,000 to 40,000 K, and log g values of 3.5, 4.0, 4.5 and 5.0 (panel a). Panel b shows the fit residuals for the different values of log g tested. The best fit to the ELS data is found for T_{eff} = 31,000$\pm$1,500 K and log g = 4.8$\pm$0.2, which gives A_v = 1.16$\pm$0.03. This then gives E(B–V)=0.36$\pm$0.02, $(B-V)_0$=–0.22$\pm$0.02 and $(U-B)_0$=–1.05$\pm$0.02. These new values correspond almost exactly to those of a B0 star (Deutschman, Davis & Schild 1976).

The value for A_v is noticeably lower than previous determinations, lower even than that of F92 (A_v=1.26$\pm$0.06). The JHK data used by F92 was actually obtained around 2 months later than the Stromgren points, and this non-simultaneity may be the cause of the poor fit. Our values for the fluxes of X Per in the UBVJHK bands are obtained from observations throughout the ELS, and we are confident that our revised values are a truer representation of the flux distribution of X Per. We note that our best fit parameters for T_{eff} and log g are very similar to those of Lyubimkov et al. (1996), who also identify X Per as a dwarf, rather than a giant as in previous classifications.

The data are dereddened using the coefficients derived above and the relationships of Rieke & Lebofsky (1985). In Fig. 3 we present an optical colour-colour plot (U–B against B–V) and

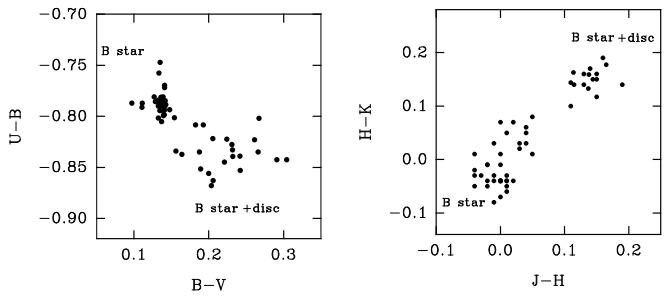

Fig. 3. Colour-colour diagrams for the X Per photometry, clearly showing the redder colours of the system when the disc is present.

an IR version (J–H against H–K). In both cases, the location of the OB star is clear, with the presence of a disc resulting in significantly redder colours.

3.2. Flux distribution

Fig. 4 shows flux-flux plots of X Per in the UBVJHK bands - plots for the RILM bands are very similar, but are not shown because of the greater scatter and the incomplete coverage of the observations. These plots all demonstrate the clear linear dependence of the flux variations. This is evidence for only *one source of variability* in the system. Choloniewski (1981) showed that in this case the energy distribution of the variable source remains unchanged in spite of the changing total luminosity. Whilst we cannot exclude the possibility that the primary star itself is variable to some small degree, we note that the lack of any measurable changes in the first two years of the ELS (Percy, 1992) places an upper limit on the degree of any such variability. We therefore associate the observed flux variations with the varying envelope only.

In Fig. 5 we show the flux density distribution of X Per. We have plotted the expected flux density of a B0V star from Kurucz models (1979, 1993) (solid line) as a comparison with the ELS observations (solid circles). Reasonable agreement is seen in all bands from U to L, suggesting that our ELS photometry is truly representative of the naked OB star, with little measurable contribution from an envelope. In order to estimate the flux distribution of the variable envelope emission, we simply determine the slopes of the dependencies from Fig. 5, which correspond to the ratios of the fluxes of the variable source in the corresponding wavelengths, as shown by Choloniewski (1981). The resulting flux distribution (solid triangles) is close to a black body at around 6200K in the range from V to L, with marked excess radiation shortwards from V. The shape of this distribution remains constant during all of the periods when an envelope appears to be present, and is independent of whether X Per is brightening or fading. Within our observational limits, there is no evidence for any other variable component in this system.

Fig. 6 summarises our observations of the recent changes in X Per on a plot of absolute magnitude against intrinsic colour, $(B–V)_0$. We find a distance of 900pc$\pm$300pc is required to fit our data to a B0V star, consistent with the recent distance estimate of

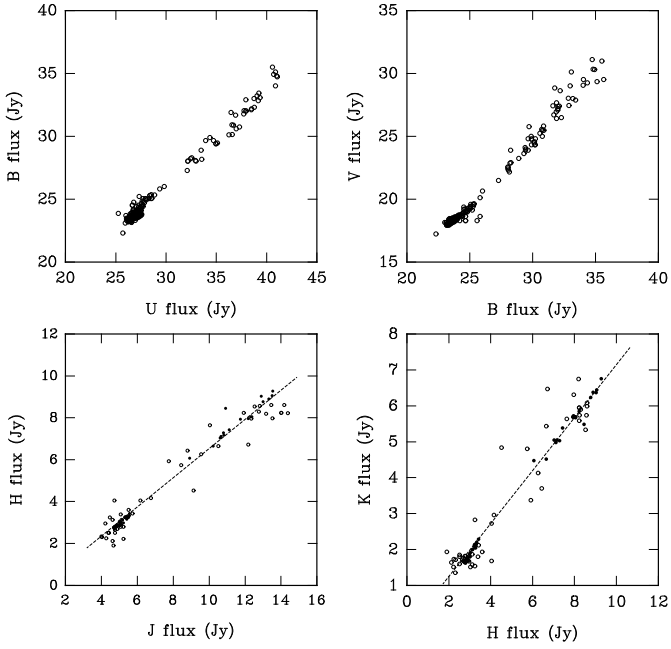

Fig. 4. Sample flux-flux diagrams for the dereddened X Per photometry. In the infrared figures, filled circles are data obtained from the 1.5m TCS on Tenerife, open circles are observations from other sources.

Lyubimkov et al. (1996), d=700pc$\pm$300pc, and also the earlier estimates of 1300pc$\pm$400pc (N91; F92; R93). The cluster of points around the brightness minimum represents the naked OB star, and we note that it is the large amplitude of the observed changes which is atypical of Be-type stars (e.g. $\Delta V = 0.6$ mags.). Further discussion of this is left to the modelling paper (Telting et al. 1996), but it appears that X Per's anomalous behaviour may be linked to an unusually dense circumstellar disc.

4. Polarimetry

4.1. Observations

The Crimean observations were carried out with the 1.25m telescope with a five channel UBVRI photometer-polarimeter made by Helsinki University Observatory (Piirola 1973). It obtains simultaneous measurements in the five colour bands with effective wavelengths 0.36, 0.44, 0.53, 0.69 and 0.83μm, near the standard UBVRI system. For photometry, we used the comparison star HD 24167. Before analyzing the polarimetric data, they were corrected for instrumental polarization using check stars from the list of Serkowski, Mathewson and Ford (1975).

The bulk of the observations were carried out between November 1993 to December 1994 (Table 2), but three polarimetric measurements were obtained in December 1992 to January 1993 when the star was in the optical low state (Table 3). Listed are the Stokes parameters (q,u) with their respective errors (from quantum statistics), and a column containing the Julian and Civil dates for the observations, with n, the number of observations made each night.

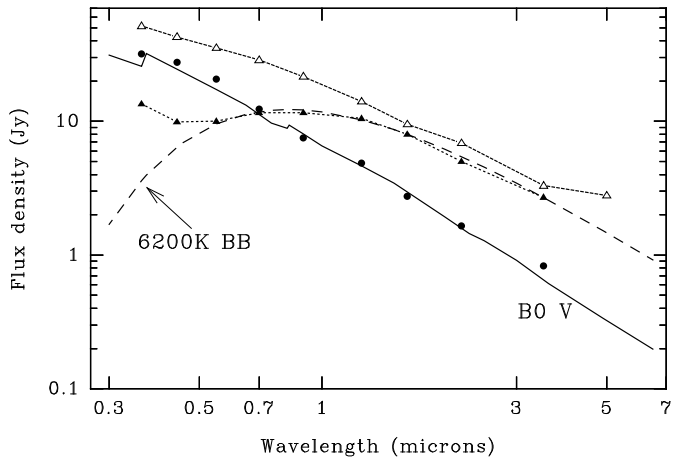

Fig. 5. The flux density against wavelength for X Per during the ELS (solid circles) and the preceding bright state (open triangles), shown with the Kurucz model for a B0V star (solid line). The closed triangles represent the variable component (assumed to be the envelope), its relative flux density distribution remaining the same during the past decade. A reasonable fit is obtained from the V to L bands with a simple black body curve of 6200K.

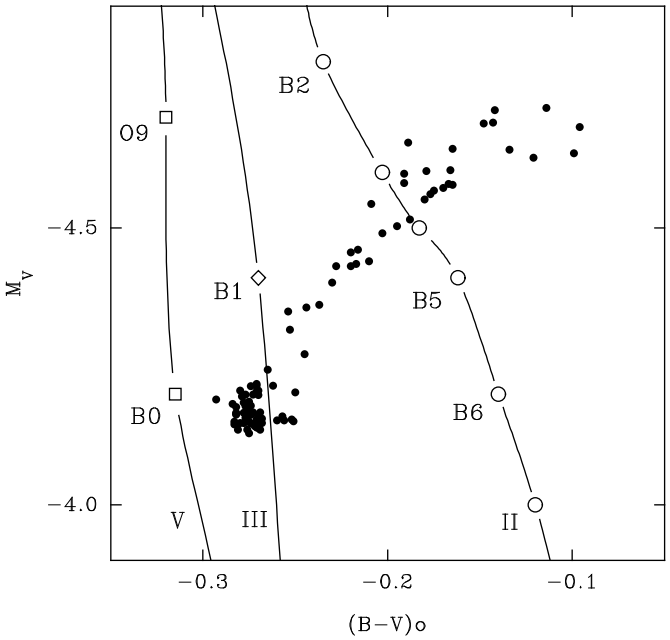

Fig. 6. The absolute magnitude M_V against intrinsic B–V colour plot, asssuming a distance of 900pc to fit the B0V classification. The data for main sequence (V), giant (III) and bright giants (II) from Deutschman, Davis & Schild (1976) are shown for comparison. The location of the naked OB star, and the direction and amplitude of variability associated with X Per is clearly seen. Whilst the direction of variability is merely a function of inclination, the large amplitude is very unusual.

4.2. Interstellar polarization

A detailed study of the stellar polarimetry requires knowledge of the value of the interstellar polarization (P_{IS}). According to Kemp and Barbour (1983) the value of interstellar polarization for X Per is very uncertain. The star is located in a region of the sky with large scattering in polarization value and position angle. They obtained P_{IS} near 0.9% and θ_{IS} near 45° in the V band. Clarke and McGale (1988) re-analyzed the Kemp and Barbour data, adding more data but for a wider (±5°) sky region, and obtained P_{IS}=0.99%(±0.16%) and θ_{IS}=69°±11°.

Clarke and McLean (1975) estimated P_{IS} by using values of depolarization in the Hydrogen emission lines of X Per, and obtained P=0.78%±0.07%, θ=57°±3° and 0.82°±0.11°, 55°±3° for Hα and Hβ respectively.

Our polarimetric data confirm the conclusion of Kemp and Barbour (1983) and Clarke and McGale (1988) that variability of linear polarization in X Per has identifiable eigendirections, suggesting that the polarimetric behaviour is related to some preferred axis.

Fig. 7 displays the data of KH95 combined with our observations. It is clear that there is no systematic shift between these datasets, so our analysis utilises both. We first assume that the direction of maximum scatter in these plots is that of the intrinsic polarization due to scattering within the circumstellar envelope. Combining the datasets, we obtain θ_{INT}=171°±0.7°. We must now make some assumptions concerning the location of the interstellar polarization vector.

If the location of the interstellar polarization were within the body of the data, we should observe a 90° rotation of the intrinsic polarization vector, which is not expected from any existing Be star models. The intrinsic polarization cannot be located in the lower right corner (i.e. high q, low u), as this would contradict the observational evidence for the ELS (absence of Hα emission and IR excess). Therefore, we are left to conclude that the interstellar polarization must lie in the upper left corner of the plots.

We will now derive a more accurate value for the interstellar polarization by combining our photometric and polarimetric data. We have previously shown that the magnitudes observed in the ELS correspond to the naked B star, and hence near-zero intrinsic polarization (assuming the polarization of the B star is negligible). Fig. 8 shows plots of the polarized flux in each band (UBVRI) against total flux, with the minimum light flux from the ELS marked in each case. The full process for calculating the interstellar polarization is detailed in the Appendix. By this method, we obtain the values for the interstellar polarization towards X Per given in Table 4. The values of KH95 are shown for comparison. Note that the quoted errors for our values are only the formal errors generated by fitting our simple model to the dependencies of Serkowski, Mathewson and Ford (1975).

Fig. 10 shows the wavelength dependence of our interstellar polarization values, fitted with the empirical relationship of Serkowski, Mathewson & Ford (1975) in the form:

$$P_\lambda = P_{\max}\ exp[-2.07\ \lambda_{\max}\ ln^2(\lambda/\lambda_{\max})]$$

Table 2. Polarimetric results obtained after the end of the ELS, whilst X Per was brightening.

Filter	q / %	error	u / %	error	Comments
U	-0.112	0.035	0.593	0.023	2449311.36
B	0.085	0.033	0.708	0.005	19-11-93
V	0.064	0.018	0.811	0.032	(n=4)
R	0.022	0.019	0.775	0.028	
I	0.041	0.022	0.716	0.028	
U	-0.070	0.019	0.609	0.028	2449320.42
B	0.095	0.022	0.729	0.042	28-11-93
V	-0.010	0.029	0.831	0.056	(n=16)
R	-0.064	0.025	0.876	0.052	
I	-0.072	0.041	0.786	0.049	
U	-0.112	0.011	0.677	0.010	2449327.19
B	0.034	0.009	0.692	0.008	05-12-93
V	0.050	0.010	0.802	0.009	(n=94)
R	-0.001	0.008	0.808	0.008	
I	-0.021	0.010	0.725	0.008	
U	-0.087	0.031	0.614	0.023	2449351.31
B	-0.002	0.028	0.697	0.027	29-12-93
V	-0.002	0.025	0.810	0.024	(n=24)
R	-0.024	0.037	0.818	0.029	
I	-0.032	0.032	0.705	0.031	
U	-0.039	0.019	0.647	0.028	2449354.42
B	0.077	0.022	0.747	0.042	1-1-94
V	0.023	0.029	0.864	0.056	(n=14)
R	-0.021	0.035	0.865	0.061	
I	-0.044	0.040	0.811	0.074	
U	-0.004	0.016	0.607	0.019	2449357.30
B	0.110	0.017	0.743	0.013	04-01-94
V	0.073	0.011	0.826	0.012	(n=48)
R	0.080	0.035	0.802	0.021	
I	-0.006	0.023	0.759	0.017	
U	-0.104	0.011	0.573	0.014	2449361.30
B	0.053	0.010	0.684	0.009	08-01-94
V	0.025	0.009	0.781	0.013	(n=44)
R	-0.022	0.014	0.766	0.014	
I	-0.069	0.017	0.759	0.016	
U	-0.061	0.024	0.678	0.026	2449375.28
B	0.057	0.023	0.795	0.027	22-01-94
V	0.053	0.029	0.883	0.030	(n=32)
R	0.007	0.068	0.940	0.057	
I	0.047	0.058	0.883	0.052	
U	-0.067	0.016	0.644	0.019	2449404.28
B	0.050	0.017	0.794	0.020	20-02-94
V	0.057	0.024	0.901	0.024	(n=48)
R	-0.066	0.034	0.936	0.048	
I	-0.046	0.039	0.885	0.046	

4.3. Intrinsic polarization

Fig. 9 also shows the wavelength dependence of intrinsic polarization over the various stages of the X Per light history. Line 1 is the mean of 4 observations from the fading stage. Lines 2 and 3 again correspond to the mean of 4 observations, this time obtained in the ELS. Line 4 corresponds to the mean of 5 observations obtained during the brightening stage. For comparison, the model estimates of Poeckert & Marlborough (1978) for Be-

Table 3. Polarimetric results from ELS.

Filter	q / %	error	u / %	error	Comments
U	-0.272	0.021	0.560	0.026	2448958.37
B	-0.242	0.017	0.717	0.019	01-12-92
V	-0.247	0.014	0.870	0.030	(n=10)
R	-0.257	0.027	0.883	0.026	
I	-0.176	0.021	0.803	0.030	
U	-0.263	0.010	0.592	0.030	2448959.36
B	-0.192	0.024	0.795	0.021	02-12-92
V	-0.175	0.031	0.846	0.026	(n=7)
R	-0.189	0.013	0.917	0.028	
I	-0.146	0.016	0.822	0.009	
U	-0.116	0.037	0.770	0.018	2448992.26
B	-0.339	0.031	0.836	0.026	04-01-93
V	-0.376	0.039	0.985	0.056	(n=4)
R	-0.235	0.031	0.963	0.033	
I	-0.106	0.064	0.965	0.052	

Table 4. Derived values for the interstellar polarization from this paper and the values of Kunjaya & Hirata (1995) for comparison.

	$P_{\rm IS,max}/\%$	$\lambda_{\rm max}$ / μm	$\theta_{\rm IS,max}$ / $^\circ$
This paper	1.24 ± 0.01	0.62 ± 0.01	60 ± 1
KH95	1.07 ± 0.18	0.65 ± 0.06	57 ± 3

star envelopes are also included. Clearly, our results contradict the predictions of the Poeckert & Marlborough (1978) model. A similar situation was noted by KH95, and our additional data and new method of determining interstellar polarization confirm this. We also note that observations of another BeXRB, A0535+262, by Larionov (in preparation) result in very similar wavelength dependencies.

Fig. 10 shows the variation of intrinsic V band polarization with time, plotted with the V photometric lightcurve. It is is clear that there is close agreement between the two, confirming that polarization arises in the same elongated envelope that is the source of IR excess radiation and emission lines.

5. Discussion

We have presented the optical and IR photometric history of X Per over the past 10 years, a period spanning a phase change from Be to OB and back to a Be star. We have derived values for the intrinsic colours of the OB star which differ slightly from the values found previously, E(B–V)=0.36±0.03 and A_v =1.16±0.02, $(B\text{-}V)_0$=-0.22±0.03 and $(U\text{-}B)_0$=-1.05±0.04, implying a B0V star at a distance of 900±300pc. Our datasets cover a far greater span of both time and wavelength than those of F92 (derived from a single set of non-simultaneous Stromgren *ubvyβ* and JHK photometry), and are thus more reliable.

We find only one source of variability in the system, which we associate with the circumstellar envelope. The OB star itself appears to display an unusual lack of variability during the ELS. The dereddened flux density distribution of the variable component matches that expected from a Blackbody at around 6200K. The behaviour of this variable component appears in some ways typical of that expected from a Be star (e.g. the reddening asso-

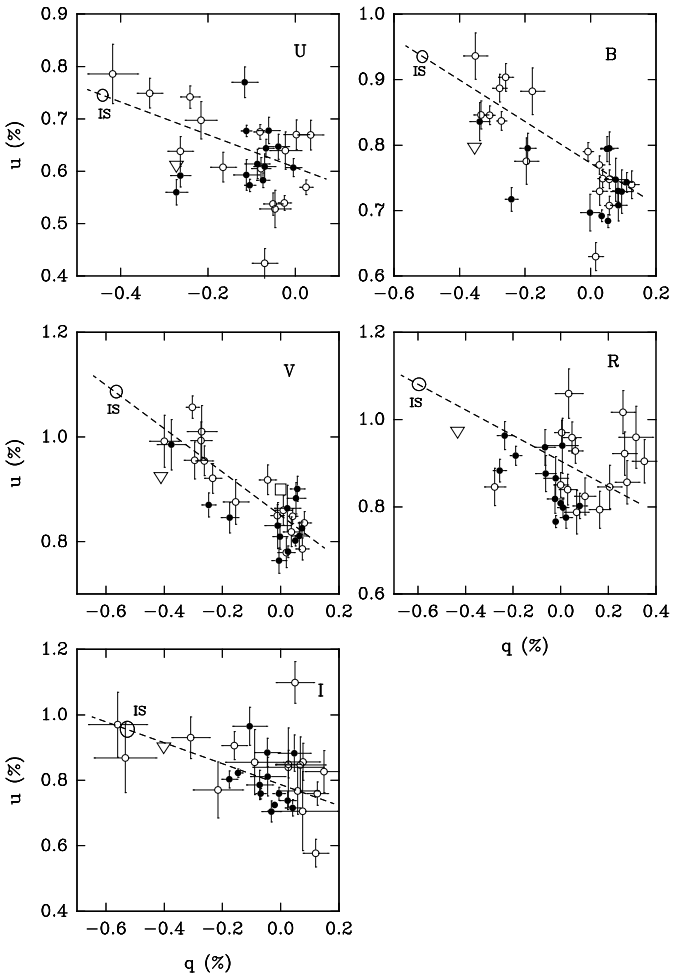

Fig. 7. Stokes parameters (q,u) plotted for each of the UBVRI bands. Data are from this paper (closed circles) and KH95 (open circles), showing good agreement. The location of the intrinsic polarization line (dashed line) and the calculated interstellar polarization point (large circles) are shown for each band. Also shown are the interstellar polarization points of previous authors, those of KH95 in each band (open triangles) and the V band point of Kemp & Barbour (1983) (open square). The values of Clarke & McGale (1988) fell outside the plot.

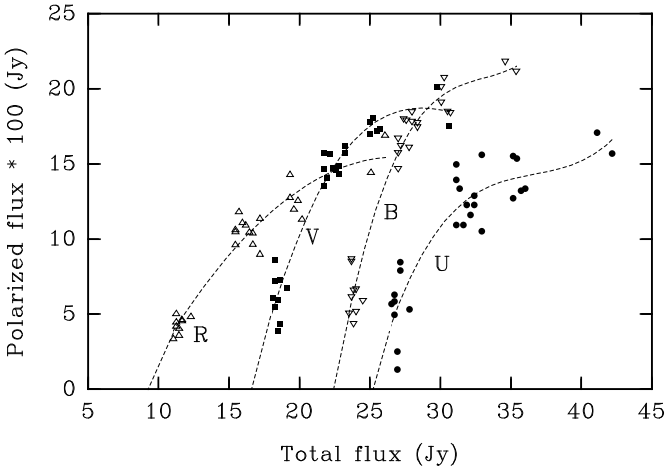

Fig. 8. Polarized flux in the UBVR bands against total flux and best fit lines.

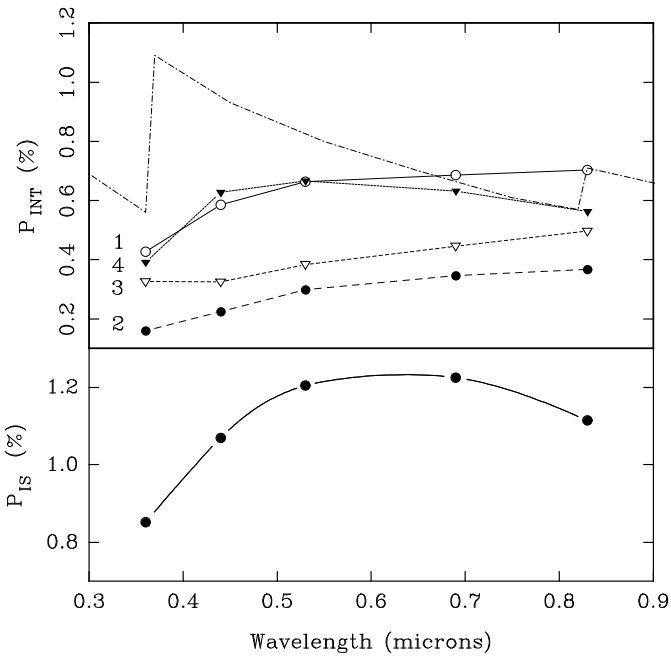

Fig. 9. Wavelength dependence of the calculated intrinsic and interstellar polarization values. Also shown is the expected wavelength dependence of the envelope polarization from the Poeckert & Marlborough (1978) model (dot dashed line).

ciated with envelope expansion, the wavelength dependence of the amplitude of flux variations and the direction of variability on Fig. 6, which is related to the inclination), but it is the large amplitude of the observed changes which is very unusual (e.g. ΔV$\approx$0.6 mags).

We have estimated the intrinsic and interstellar polarization parametes of X Per, and find that polarization arises as a result of light scattering in the same disc which is responsible for the excess radiation and the emission lines. The measured differences between the observed polarizations and those expected from models of the disc structure could be a result of the disc geometry (e.g. if there is a strong radial dependence of the discs' geometrical and optical thickness). Geometrical effects might also be responsible for the unusually large amplitude of both polarization and brightness variations. Further discussion and modelling of these data will be presented in later papers.

Acknowledgements. We wish to thank those involved with making the observations of X Per over the past years, particularly Chris Everall, Sarah Unger, Gemma Capilla and Jose Miguel Torrejon. We are again indebted to the BAA VSS, whose monitoring of X Per has proved invaluable over the years. Data reduction was carried out at the Southampton and Sussex STARLINK nodes, funded by the UK PPARC. We are grateful to the Crimean Astrophysical Observatory, UK PATT and Spanish CAT for awarding telescope time for these observations. The TCS is operated by the Instituto de Astrofisica de Canarias in the Teide Observatory. VL and LL were supported by Russian Federal Program "Astronomy" grant 2-235 and RFFI grant 96-02-19703. PR acknowl-

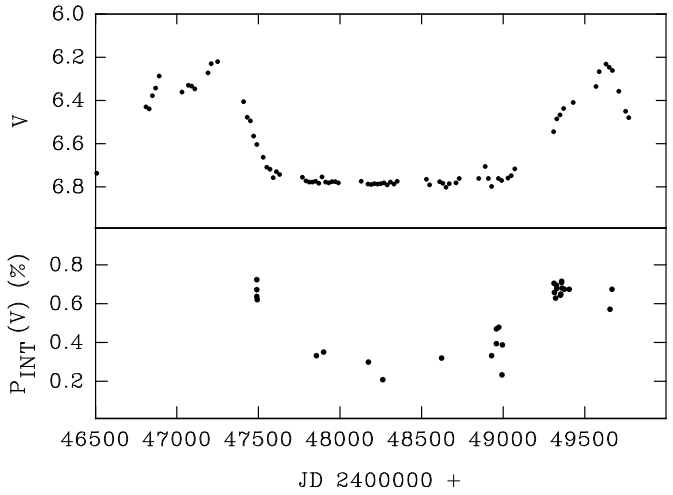

Fig. 10. Variation of V band intrinsic polarization with time, plotted with the V lightcurve. A strong correlation is evident.

edges receipt of a Nuffield Foundation grant to newly qualified lecturers. AET, VL and LL are grateful for the receipt of funding from a PPARC visitors grant to undertake work at Sussex. JSC acknowledges receipt of a PPARC studentship, IN is supported by a grant from the Univ. of Southampton.

Appendix: determination of interstellar polarization

The technique used by Larionov to derive the value of the interstellar polarization requires that we have simultaneous (or near-simultaneous) photometry and polarimetry, and further develops the technique first proposed by Hagen-Thorn (1981).

We make a number of assumptions for our model, the main one being that the total radiation is the sum of a constant source of radiation (e.g. a normal star) whose flux can be estimated by some means (in this case by the lack of an infrared excess and by minimum brightness associated with the disc loss), and a variable source of polarized radiation (scattering of radiation by the envelope).

In this case, the observational points would be located along the intrinsic line. To determine the interstellar polarization, we first take an arbitrary point (q'_{IS}, u'_{IS}) lying somewhere on the intrinsic polarization line, outside of the region occupied by the observational points. We then calculate our preliminary estimate for the intrinsic polarization (p'_i) value for each date and multiply it by the total flux (F_i) at that time derived from our photometry. It is evident that our preliminary value of intrinsic polarization differs from the 'true' value, (p_i), by an additive constant (c), so that

$$p'_i = p_i + c \tag{1}$$

The polarized flux obtained this way is plotted against the total flux. We must then fit the dependence:

$$p'_i F_i = f'(F_i) \tag{2}$$

so that it intersects the abscissa at the point where $F_i = F_0$, where F_0 is the flux of the constant source (see Fig.9).

In the simplified case of a linear dependence we can rewrite (2) as:

$$(p'_i - c)F_i = k(F_i - F_0) \tag{3}$$

where k is the slope of the dependence. Solving this overdetermined system of n equations, where n is the number of data points, we obtain the values of c and k.

We can then obtain the 'true' value of the interstellar polarization by:

$$q_{IS} = q'_{IS} - c\cos 2\theta_{INT}$$

and

$$u_{IS} = u'_{IS} - c\sin 2\theta_{INT}$$

As a rule, this procedure should be carried out at least twice because of the scatter of the data points around the intrinsic line.

References

Braes, L.L.E. & Miley, G.K., 1972, Nat, 235, 273
Brucato, R.J. & Kristian, J., 1972, ApJ, 173, L105
Choloniewski, J., 1981, Acta Astronomica, 31, 3, 293
Clark, J.S., Roche, P., Steele, I.A., et al., 1996, in preparation
Clarke, D. & McLean, 1975, MNRAS, 173, 21
Clarke, D. & McGale, P.A., 1988, A&A, 190, 93
Corbet, R. & Thomas, B., 1991, IAU Circ. 5372
Deutschman, W.A., Davis, R.J. & Schild, R.E., 1976, ApJS, 30, 97
Fabregat, J., Reglero, V., Coe, M.J. et al., 1992, A&A, 259, 522
Gottlieb, E.W., Wright, E.L. & Liller, W., 1975, ApJL, 202, L13
Hagen-Thorn, V.A., 1981, Trudy Astronomicheskoy Observatorii Leningradskogo Universiteta, 36, 20
Hang Heng-rong & Zang Zhi-yun, 1994, Publ. of the Purple Mountain Observatory, no.4 , 13
Hudec, R. & Ratz, K., 1989, Proc. 23rd ESLAB Symp. on Two Topics in X-ray Astronomy, Bologna, Italy, ESA SP-296, 427
Hutchings, J.B., Crampton, A.P. & Redman, R.O., 1975, MNRAS 170, 313
Kemp, J.C. & Barbour, M.S., 1983, ApJ, 264, 237
Kunjaya, C. & Hirata, R., 1995, PASJ, 47, 589
Kurucz R.L., 1979, ApJS 40, 1
Kurucz R.L., 1993, CD-ROM No. 13
Lyubimkov, L.S., Rostopchin, S.I., Roche, P. & Tarasov, A.E., 1996, A&A submitted
Mook, D.E., Boley, F.I., Foltz, C.B. & Westphfal, D., 1974, PASP, 86, 894
Norton, A.J., Coe, M.J., Estela, A. et al., 1991, MNRAS, 253, 579
Percy, J., 1992, JAAVSO, 21, 29
Piirola, V., 1973, A&A, 27, 383
Poeckert, R. & Marlborough, J.M., 1978, ApJ, 220, 940-961
Rieke, G.H. & Lebofsky, M.J., 1985, ApJ, 288, 618
Robba, N.R. & Warwick, R.S., 1989, ApJ, 346, 469
Roche, P., Coe, M .J., Fabregat, J. et al., 1993, A&A, 270, 122
Roche, P., Tarasov, A.E., Chakrabarty, D., et al., 1996, in preparation
Serkowski, K., Mathewson, D.S. & Ford, V.L., 1975, ApJ, 196, 261
Tarasov, A.E. & Roche, P., 1995, MNRAS, 276, L19
Telting, J.H., Waters, L.B.F.M, Roche, P., et al., 1996, in preparation
Turner, D.G., 1990, PASP, 102, 1331
van den Bergh, S., 1972, Nat, 235, 273
Weisskopf, M.C., Elsner, R.F., Darbo, W. et al., 1984, ApJ, 278, 711
White, N.E., Mason, K.O., Sanford, P.W. & Murdin, P., 1976, MNRAS, 176, 201
Zamanov, R.K. & Zamanova, V.I., IBVS 4189